Supplementary data for article:

Bjelogrlić, S. K.; Todorović, T.; Cvijetić, I.; Rodić, M. V.; Vujčić, M.; Marković, S. B.; Araškov, J.; Janović, B.; Emhemmed, F.; Muller, C. D.; et al. A Novel Binuclear Hydrazone-Based Cd(II) Complex Is a Strong pro-Apoptotic Inducer with Significant Activity against 2D and 3D Pancreatic Cancer Stem Cells. *Journal of Inorganic Biochemistry* **2019**, *190*, 45–66. https://doi.org/10.1016/j.jinorgbio.2018.10.002

Supplementary material

A novel binuclear hydrazone-based Cd(II) complex is a strong pro-apoptotic inducer with significant activity against 2D and 3D pancreatic cancer stem cells

Snežana Bjelogrlić[a,b], Tamara R. Todorović[c], Ilija Cvijetić[d], Marko V. Rodić[e], Miroslava Vujčić[f], Sanja Marković[c], Jovana Araškov[c], Barbara Janović[f], Fathi Fathi Emhemmed[b], Christian D. Muller[b], Nenad R. Filipović[g,*]

[a]*National Cancer Research Center of Serbia, Pasterova 14, Belgrade, Serbia*

[b]*Institut Pluridisciplinaire Hubert Curien, UMR 7178 CNRS Université de Strasbourg, 67401 Illkirch, France*

[c]*Faculty of Chemistry, University of Belgrade, Studentski trg 12-16, Belgrade, Serbia*

[d]*Innovation Center of the Faculty of Chemistry, University of Belgrade, Studentski trg 12-16, Belgrade, Serbia*

[e]*Faculty of Sciences, University of Novi Sad, Trg Dositeja Obradovića 3, Novi Sad, Serbia*

[f]*Institute of Chemistry, Technology and Metallurgy, University of Belgrade, Njegoševa 12, Belgrade, Serbia*

[g]*Faculty of Agriculture, University of Belgrade, Nemanjina 6, Belgrade, Serbia*

*Corresponding author

Nenad R. Filipović, PhD

E-mail: nenadf.chem@gmail.com; nenadf@agrif.bg.ac.rs

Table of contents

Experimental part

Solution studies

All NMR spectral measurements were performed on a Bruker Avance III 500 spectrometer equipped with a broad-band direct probe. The spectra were recorded at room temperature in DMSO-d_6. Chemical shifts are given on δ scale relative to tetramethylsilane as internal standard for ^{1}H and ^{13}C or $Cd(ClO_4)_2$ in D_2O as external standard for ^{113}Cd. Coupling constants (*J*) were expressed in Hz. Abbreviations used for NMR spectra: s, singlet; d, doublet; t, triplet; br. broad. 1D and 2D spectra are shown in Figures S2–S11. UV-visible (UV-Vis) spectrum was recorded on a GBC Scientific Cintra 6 UV-Vis spectrophotometer (200-1000 nm), using sample dissolved in DMSO (Figures S12).

Calculation of electronic spectral data

The Gaussian 09 program suite [S1] was used for the quantum mechanical computations. Molecular structures were optimized using density functional theory (DFT) approach, with B3LYP [S2,S3] functional in the gas phase, and re-optimized in dimethyl sulfoxide (DMSO) solvent, stimulated by the universal solvation model (SMD) [S4]. The cadmium ion was described using the lanl2dz EPC [S5] and for all other atoms 6-31G(d,p) [S6,S7] basis sets were applied. The calculations were performed under restricted formalism, using tight convergence criteria, without any symmetry constraints and all the ground state geometries were verified by frequency calculations. To obtain the calculated UV-Vis spectra (Figure S13), the time dependent density functional theory (TD-DFT) calculation was performed, using the same functional, the basis sets and the solvent. The single crystal structure of **1** was used as starting geometries for theoretical calculations. Also, the several species, potentially present in DMSO solution, has been considered (Figure S13).

Anticancer experiments

Cell cultures

Human mammary adenocarcinoma (MCF-7, ATCC® HTB-22) and human pancreatic adenocarcinoma (AsPC-1, ATCC® CRL-1682) cell lines were maintained in DMEM high glucose medium (Dominique Dutscher, 67172 Brumath cedex, France, Cat No L0102-500), supplemented with 10% (v/v) heat inactivated fetal bovine serum (FBS, Life Technologies, Paisley, UK, Cat No 10270-106) and 1% (v/v) penicillin-streptomycin (10,000 units/mL and

10,000 µg/mL, Life Technologies, Paisley, UK, Cat No 15140-122). Cells were kept at 37 ºC in humidified atmosphere containing 5% (v/v) CO_2 during their exponential growing phase and in the course of incubation with investigated compounds.

Complex **1** was initially dissolved in dimethyl sulfoxide (DMSO) as 20 mM stock solution. Further dilutions applied in cell experiments have been done in DMEM just before each use, with a final concentration of DMSO never exciding 0.5% (v/v). CDDP was dissolved in phosphate buffer solution (PBS) while its further dilutions have been made in DMEM.

Annexin V and propidium iodide (PI) staining

Cells were seeded in 96 wells flat bottom plates (Corning® Costar®, Cat. No. CLS3596) in 0.1 mL, at a density of 10 000/well and left overnight. Investigated compounds were added in a range of six concentrations. As controls, non-treated cells, cells treated with 0.5% DMSO, and cells treated with Celastrol (Enzo Life Sciences, Cat. No. ALX-350-332-M025) at 50 µM concentration were used.

After 24 h of incubation, AsPC-1 and MCF-7 supernatant non-adherent cells were transferred into another 96 well plate. For the remaining adherent cells, 200 µL of 2 mM EDTA in 0.9% NaCl was added and plates have been left for 15 min at 37 °C. EDTA solution was discarded after plates were centrifuged at a relative centrifugal force (RCF) 450×*g* for 10 min, then 200 µL of trypsin-EDTA (BioWest, Nuaille, France, Cat No L0930-100) was added to each well. Plates were incubated for 15 min at 37 °C and supernatants were removed after additional spinning cycle. Previously removed supernatants with non-adherent cells were returned to detached cells and stained with Annexin V-FITC (Immuno Tools, Friesoythe, Germany, Cat No 31490013) and propidium iodide (PI, Miltenyl Biotec Inc, Auburn, USA, Cat No 130-093-233) in a volume of 3 µL. Described trypsinization protocol was applied each time AsPC-1 and MCF-7 cells were prepared for flow cytometry analysis, unless is stated otherwise.

Cells were analyzed on Guava® easyCyte 12HT Benchtop flow microcapillary cytometer using the dedicated InCyte® software package. Cells were classified according to AnnexinV-FITC (green fluorescence) and PI (red fluorescence) labelling on viable (double negative), pre-apoptotic (Annexin V-FITC single-stained cells), necrotic (PI single-stained cells) and advanced phases of apoptosis (double-stained cells).

Calculation of $ApoC_{50}$ concentration

Percentages of Annexin V single-stained and double-stained cells were summarized for each concentration of investigated compound. The computed percentages were charted against corresponding concentrations and $ApoC_{50}$ concentration was computed as the one that corresponds to 50 % of whole apoptotic events (early and late apoptosis) on the concentration-response curve (Figure S15). Concentration-effect curves have been plotted using asymmetric five-parameter logistic equation (GraphPad Prism 6 software).

Cell cycle analysis

Distribution of cells within phases of mitotic division has been evaluated on remaining cells after Annexin V/PI analysis, which right after the read out was finished were fixed in ethanol and left overnight at 4 °C. Before reading, plates were centrifuged at an RCF 450×*g* for 10 min, ethanol was discarded, and PBS added in a volume of 100 µL per well. Cells were stained with 50 µL of FxCycle™ PI/RNAse Staining solution (Molecular Probes, Cat. No. F10797) and incubated at 37 °C for 30 min. Plates were analyzed on Guava® easyCyte 12HT Benchtop flow microcapillary cytometer using the dedicated InCyte® software package.

Inhibition of caspase activity

Cells were treated with investigated compounds at its $ApoC_{50}$ concentration for 6 h with or without pan-caspase inhibitor carbobenzoxy-valyl-alanyl-aspartyl-[O-methyl]-fluoro methylketone (Z-VAD-fmk), Promega, Madison, USA, Cat. No. G7232). Z-VAD-fmk was added in a concentration that was previously tested and confirmed as non-toxic to cells over 6 h incubation (20 µM for AsPC-1 and MCF-7 cell lines, respectively). As controls, non-treated cells, cells treated with Z-VAD-fmk only, and cells treated with investigated compound only were used. After incubation period was ended, treated cells were carried out for Annexin V/PI staining as described above, and analyzed on Guava® easyCyte 12HT Benchtop flow microcapillary cytometer using the dedicated InCyte® software package.

The percent of apoptosis inhibited by Z-VAD-fmk co-treatment was determined using equation (S1):

$$\text{Apoptosis inhibition (\%)} = [1 - (\text{\% of apoptosis in } A \,/\, \text{\% of apoptosis in } B)] \times 100 \qquad \text{(S1)}$$

where *A* is the sample treated with Z-VAD-fmk and investigated compound at its $ApoC_{50}$ concentration, while *B* is the corresponding sample treated only with the same investigated compound applied at the same concentration.

Evaluation of caspase-8 and -9 activities

Cells were treated with investigated compound at its $ApoC_{50}$ concentration for 6 h. Following trypsinization activities of caspase-8 and -9 were assayed by means of Guava Caspase 9 SR and Caspase 8 FAM kit (EMD Millipore, Cat. No. 4500-0640) following manufacturer's instructions. Cells were analyzed on Guava® easyCyte 12HT Benchtop flow microcapillary cytometer using the dedicated InCyte® software package.

Determination of mitochondrial superoxide generation

Cells were treated over 6 h with investigated compounds in a concentration of 50 µM (MCF-7 cells) or 75 µM (AsPC-1 cells), afterwards cell were trypsinized and stained with MitoSox Red (Molecular Probes, Cat. No. M36008) according to manufacturer's recommendations. Analysis was performed on Guava® easyCyte 12HT Benchtop flow microcapillary cytometer using the dedicated InCyte® software package.

Assessment of changes in mitochondrial potential

Cells were treated over 6 h with investigated compound in concentration of 50 µM (MCF-7 cells) or 75 µM (AsPC-1 cells). After incubation was terminated, cells were trypsinized and stained with FlowCellectTM MitoDamage Kit (Merck Millipore Corporation, Darmstadt, Germany, Cat. No. FCCH100106) according to manufacturer's recommendations. Analysis has been performed Guava® easyCyte 12HT Benchtop flow microcapillary cytometer using the dedicated InCyte® software package. Cells were classified according to labeling with Annexin V-FITC (Grn-B fluorescence), MitoSense Red (Red-R fluorescence), and 7-Aminoactinomycin D (7-AAD; Red-B fluorescence).

Growth inhibition of 3D tumor models

Three-dimensional AsPC-1 and MCF-7 tumor models were made in 96 well plates (Corning, Sigma-Aldrich, St. Louis, Mo, USA, Cat No 4515). Tumors were left to grow for additional four days, afterwards investigated compounds were added in concentrations of 100, 10, and 1 µM. Evaluation has been maintained during 8-day incubation period, with media exchanged on day 4. Changes in the tumor sizes have been assessed on Celigo®

imaging cytometer (Cyntellect, Brooks Life Science Systems, Poway, CA, USA) using Celigo software. Growth rates of non-treated and treated spheroids were computed for every other day during 8-day incubation by dividing the area on the day *n* with the area on the day 0.

DNA binding experiments

Agarose gel electrophoresis

Plasmid pUC19 (2686 bp in length, purchased from Sigma-Aldrich, USA) was prepared by its transformation in chemically competent cells *Escherichia coli* (*E. coli*) strain XL1 blue. Amplification of the clone was done according to the protocol for growing *E. coli* culture overnight in LB medium at 37 °C [S8] and purification was performed using Qiagen Plasmid plus Maxi kit. Finally, DNA was eluted in 10 mM Tris-HCl buffer and stored at −20 °C. The concentration of plasmid DNA (0.512 µg/µL) was determined by measuring the absorbance of the DNA-containing solution at 260 nm. One optical unit corresponds to 50 µg mL^{-1} of double stranded DNA.

Plasmid DNA (0.5 µg) was incubated with increasing volumes of stock solution of **1** (1, 2, 3 and 4 µL) in a 20 µL reaction mixture in 40 mM bicarbonate buffer (pH 8.4) at 37 °C, for 90 min. The reaction mixtures were vortexed from time to time. The reaction was terminated by short centrifugation at an RCF 6708×*g* and addition of 5 µL of loading buffer (0.25% bromophenol blue, 0.25% xylene cyanol FF and 30% glycerol in TAE buffer: 40 mM Tris-acetate, 1 mM EDTA, pH 8.24).

The samples were subjected to electrophoresis on 1% agarose gel (Amersham Pharmacia-Biotech, Inc) prepared in Tris acetate-EDTA buffer pH 8.24. The electrophoresis was performed at a constant voltage (80 V) until bromophenol blue had passed through 75% of the gel. A Submarine Mini-gel Electrophoresis Unit (Hoeffer HE 33) with an EPS 300 power supply was used. After electrophoresis, the gel was stained for 30 min by soaking it in an aqueous ethidium bromide (EB) solution (0.5 µg mL^{-1}). The stained gel was illuminated under a UV transilluminator Vilber-Lourmat (France) at 312 nm and photographed with a Nikon Coolpix P340 Digital Camera through filter DEEP YELLOW 15 (TIFFEN, USA).

Fluorescence measurements

Calf thymus DNA (lyophilized, highly polymerized, obtained from Serva, Heidelberg) (CT-DNA) was dissolved in Tris buffer (10 mM Tris-HCl, pH 7.9) overnight at 4 °C. This stock

solution was stored at 4 °C and was stable for several days. A solution of CT-DNA in water gave a ratio of UV absorbance at 260 and 280 nm, A_{260}/A_{280} of 1.89–2.01, indicating that DNA was sufficiently free of protein. The concentration of DNA (2.86 mg mL^{-1}) was determined from the UV absorbance at 260 nm using the extinction coefficient ε_{260} = 6600 M^{-1} cm^{-1} [S9]. Compound **1** was dissolved in DMSO in concentration of 10 mM. This solution was used as stock solution.

The competitive interactions of **1** and the fluorescence probe either EB or Hoechst 33258 dye (H), with CT-DNA have been studied by measuring the change of fluorescence intensity of the probe−DNA solution after addition of **1**. Reaction mixtures containing 100 μM of CT-DNA (calculated per phosphate) in 1 mL of 40 mM bicarbonate solution (pH 8.4) were pre-treated with 1.5 μL of 1% H probe solution (28 μM final concentration) or 1 μL of 1% EB solution (25 μM final concentration) in separate experiments for 20 min and the mixture was analysed by fluorescence measurement. Then the increasing concentrations of **1** were successively added and the changes in the fluorescence intensity were measured using a Thermo Scientific Lumina Fluorescence spectrometer (Finland) equipped with a 150 W Xenon lamp. The slits on the excitation and emission beams were fixed at 10 nm. All measurements were performed by excitation at 350 nm for H dye in the range of 390−550 nm, and by excitation at 500 nm for EB in the range of 520−700 nm. The control was probe−CT-DNA solution. Complex **1** did not have fluorescence under applied conditions. The obtained fluorescence quenching data were analysed according to the Stern–Volmer equation (S2) [S10]:

$$I_0/I = 1 + K[\mathbf{1}]/[\text{CT-DNA}] \qquad \text{(S2)}$$

where I_0 and I represent the fluorescence intensities of probe−CT-DNA in absence and presence of **1**, respectively, K is quenching constant. The K value is calculated from the ratio of the slope to the intercept from the plot of I_0/I *versus* [**1**]/[CT-DNA].

Primary spectra were imported into OriginPro 9.0 and were processed by this software package.

<u>Human serum albumin (HSA) interaction experiments</u>

A stock solution of fatty acid-free HSA (<0.007 % fatty acids, *M*w = 66478 Da, Sigma; c = 1.63 × 10^{-4} M) was prepared by dissolving accurate weighted mass of HSA in freshly prepared PBS (30 mM, I = 0.15 M, pH 7.38). Millipore water was used in the preparation of

buffer solution. The stock solutions of **1** ($c = 4.42 \times 10^{-4}$ M) was prepared by dissolving the necessary amount of solid in DMSO, because of their low solubility in the buffer. For HSA-compound interaction studies, HSA solution was freshly prepared from the stock by dilution with a buffer (HSA concentration was kept constant, $c = 5 \times 10^{-7}$ M), and titrated with a compound stock solution to avoid large sample dilution. After each aliquot addition, the system was stirred and left to equilibrate for 20 min before UV-Vis absorption and fluorescence emission spectra recording.

Fluorescence measurements were performed on spectrofluorometer Fluoromax-4 Jobin Yvon (Horiba Scientific, Japan), equipped with Peltier element for temperature control and magnetic stirrer for cuvette, using quartz cell with 1 cm path length and 4 mL volume. Before the recording of the fluorescence spectrum, diluted HSA solution was filtrated using PVDF filters with 0.22 μm pore size. The temperature was kept fixed at 25 °C. An excitation wavelength was 280 nm, with 5 nm slits; emission spectra were recorded in 300–500 nm wavelength range, with 5 nm slits, and 0.1 s integration time. Background PBS signal was subtracted from each spectrum.

UV/Vis spectra were recorded on GBC Cintra 6 spectrophotometer (GBC Dandenong, Australia) using quartz cell with 1 cm path length and 4 mL volume. All spectra were recorded against the corresponding blank (1% DMSO in PBS) in the 220–550 nm wavelength range, with 500 nm/min scan speed.

Acute lethality assay

Artemia salina toxicity assay was conducted as described earlier [S11]. DMSO was used as both, initial solvent and negative control (0.25% v/v), while CDDP was used as positive control. For each concentration of the tested substances two measurements were performed. LC_{50} was defined as the concentration of a substance that causes death of 50% nauplii. DMSO was inactive under the applied conditions.

Molecular docking to HSA and DNA

The initial coordinates of **1** were taken from the experimentally determined crystal structure. Charges were assigned to all ligand atoms using semi-empirical PM6 method implemented in MOPAC2016 [S12, S13]. The affinity of **1** to three most common HSA binding sites was evaluated by taking the crystal structures of HSA co-crystallized with

ligands. The binding sites were defined selecting all amino acid residues in a radius of 12 Å around ligand and removal of ligand to make the room for docking of **1**. For binding to HSA site IB, the crystal structure of idarubicin complex was used (PDB code 4LB2). For binding site IIA, a complex of HSA with indolamide derivative was used (PDB code 3LU7). Diflunisal co-crystallized with HSA (PDB code 2BXE) was used for assessing the affinity of **1** toward binding site IIIA.

The high-resolution DNA duplex sequence d(CGCGAATTCGCG)$_2$ (PDB code: 3U2N) was chosen for docking of **1** into the DNA. All ligands and water molecules were removed and the large box size was chosen, leaving the possibility for docking of **1** into both the major and minor DNA groove.

PLANTS (Protein-Ligand ANT System) [S14, S15] software was used for docking of compound **1** to HSA and DNA. The binding affinity was assessed using ChemPLP scoring function [S16]. Ten docking solutions were calculated for each binding site of HSA. For DNA binding, 20 best poses were selected and analyzed. Vega ZZ 3.1.0 [S17] was used as GUI for all calculations.

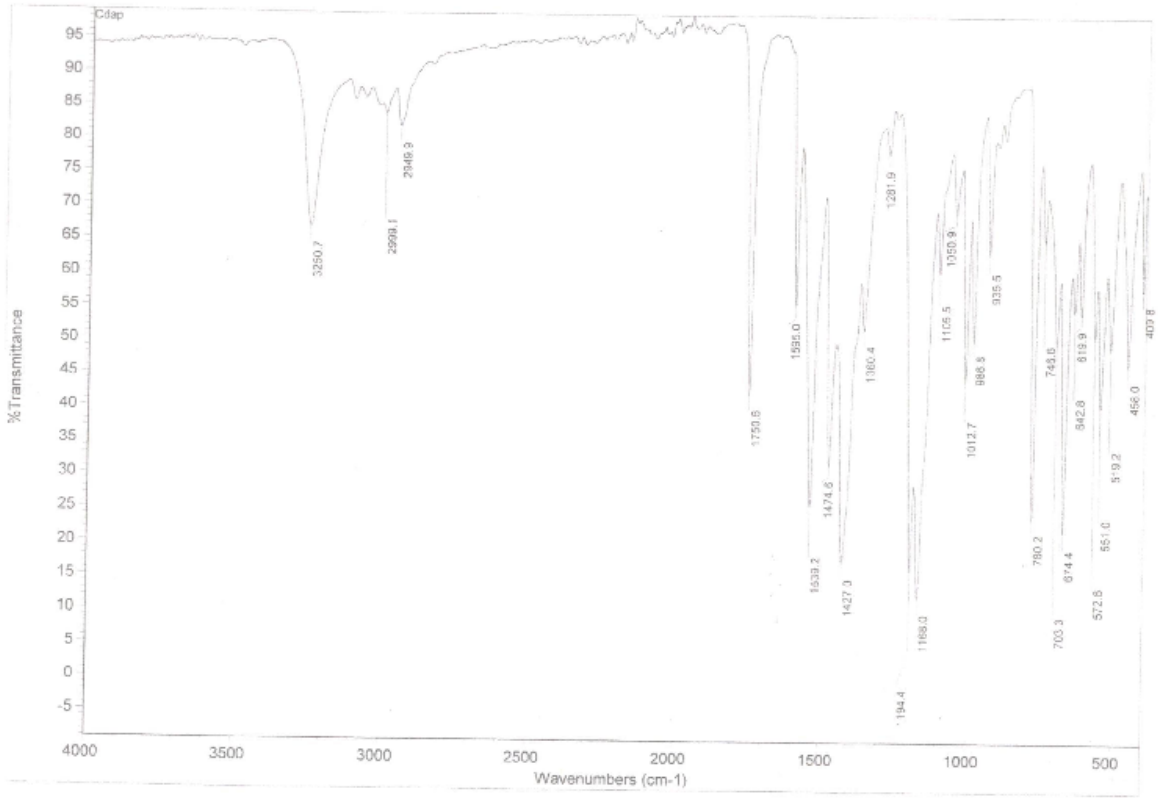

Figure S1. IR spectrum of **1**.

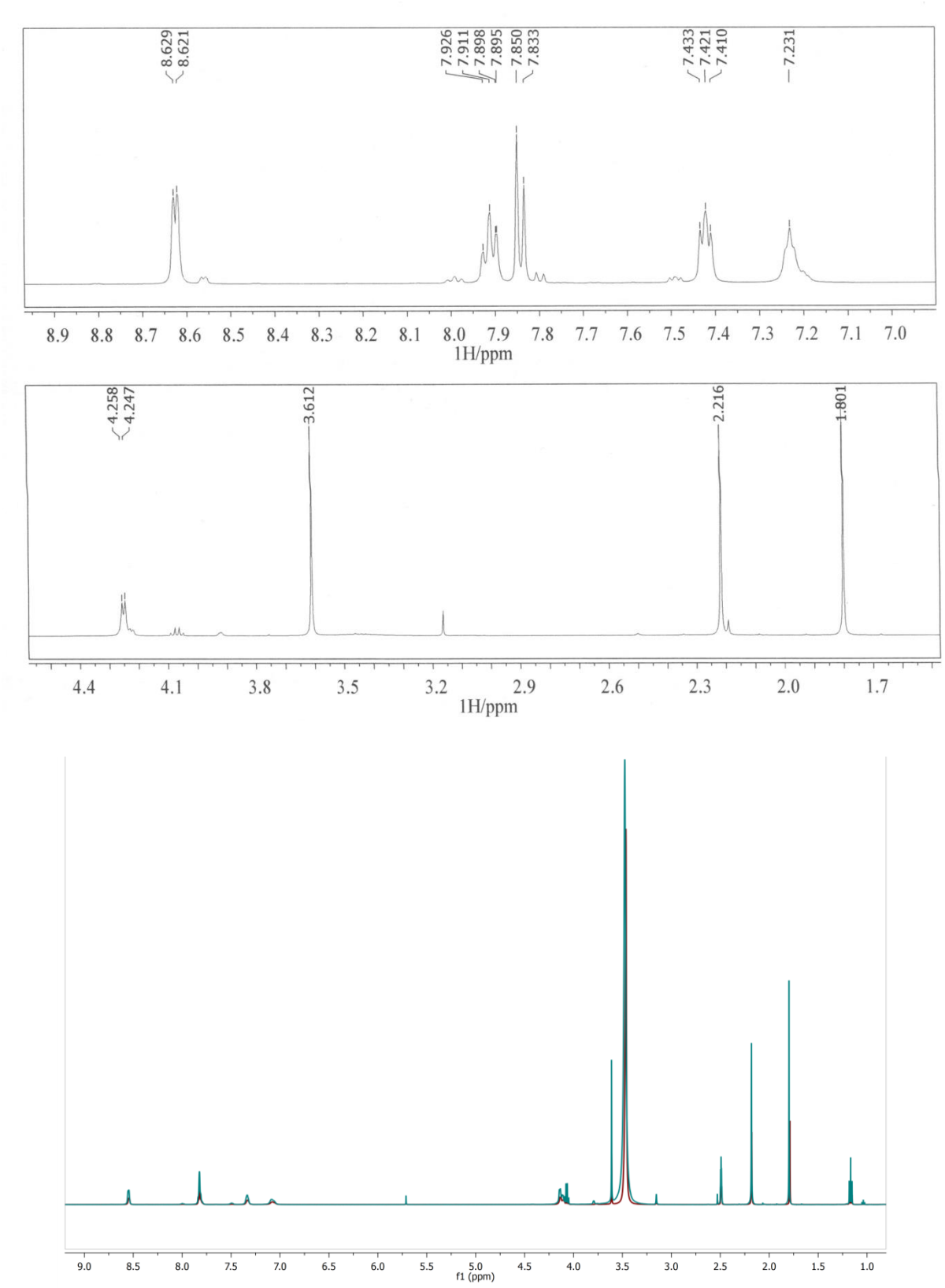

Figure S2. ^{1}H NMR spectrum of **1** in DMSO-d_6 (top and middle) and superimposed spectrum of ^{1}H NMR spectra (bottom) of freshly prepared solution of **1** (red) and after 48 h (blue).

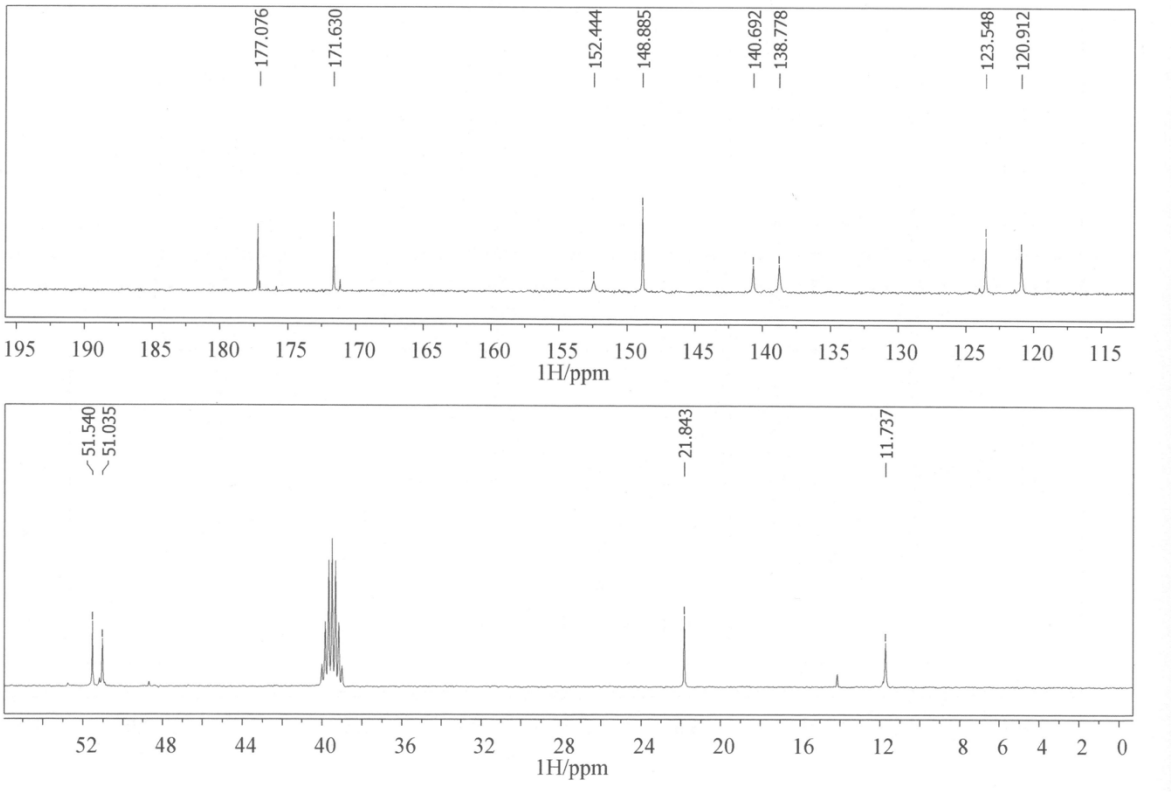

Figure S3. ^{13}C NMR spectrum of **1** in DMSO-d_6.

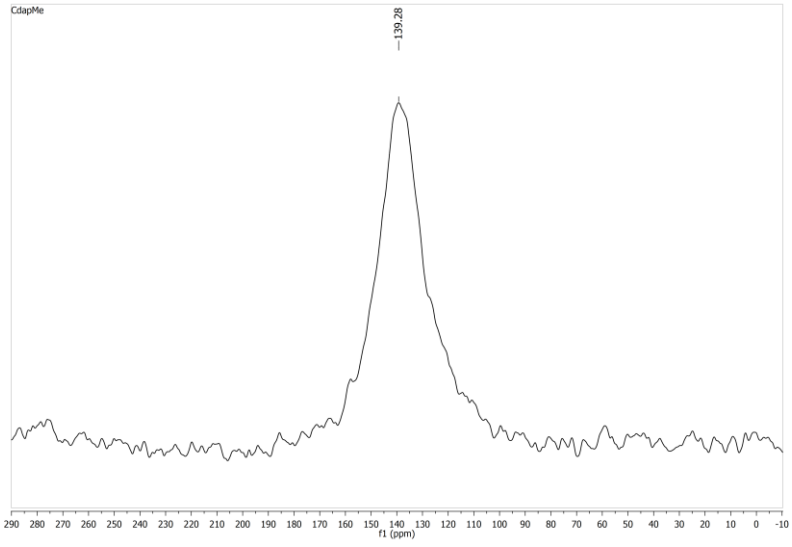

Figure S4. ^{113}Cd NMR spectrum of **1** in DMSO-d_6

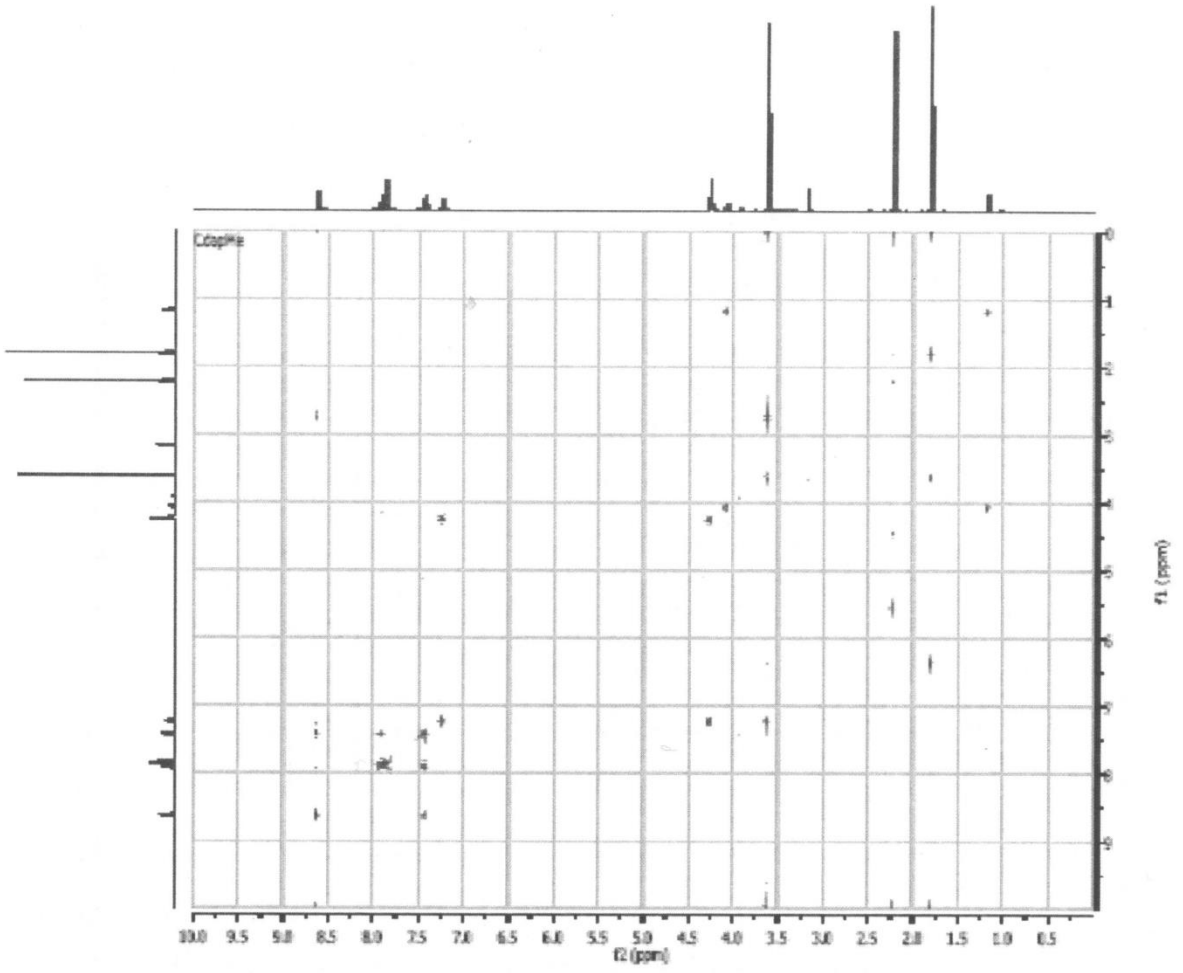

Figure S5. COSY spectrum of **1** in DMSO-d_6.

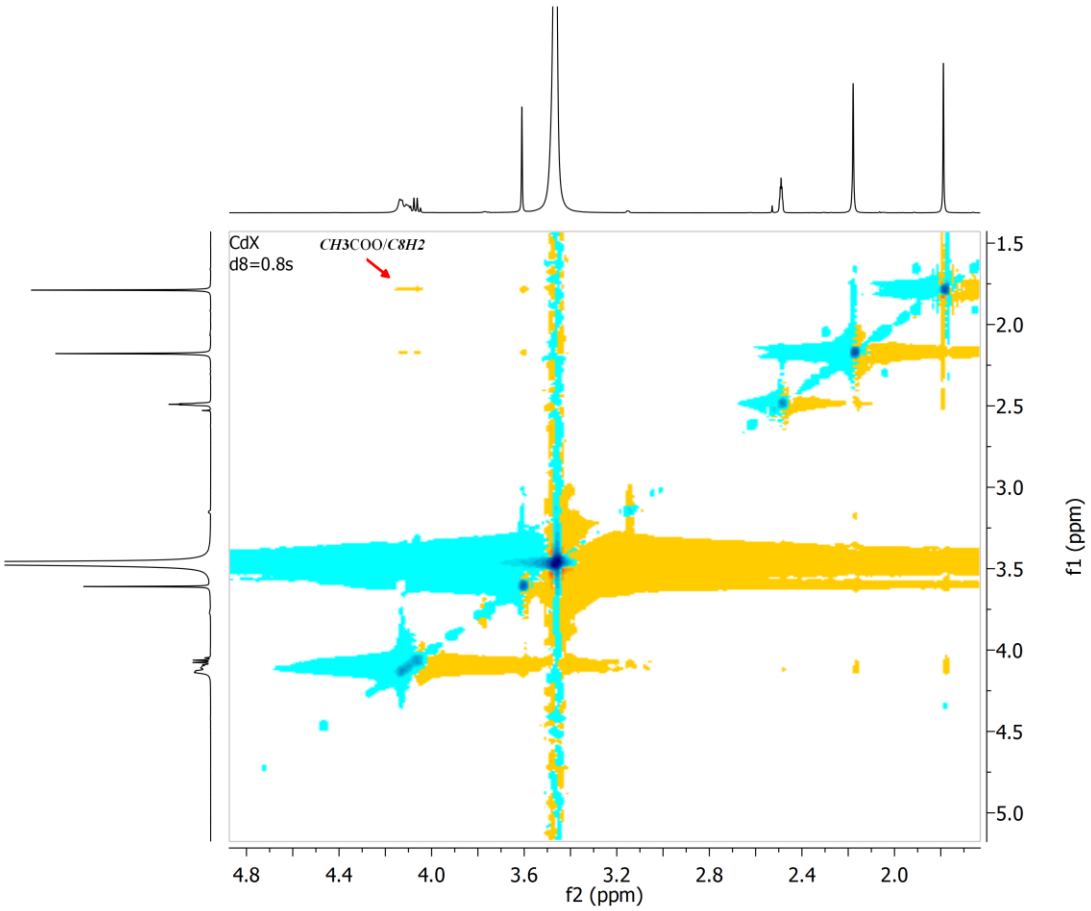

Figure S6. NOESY spectrum of **1** in DMSO-d_6

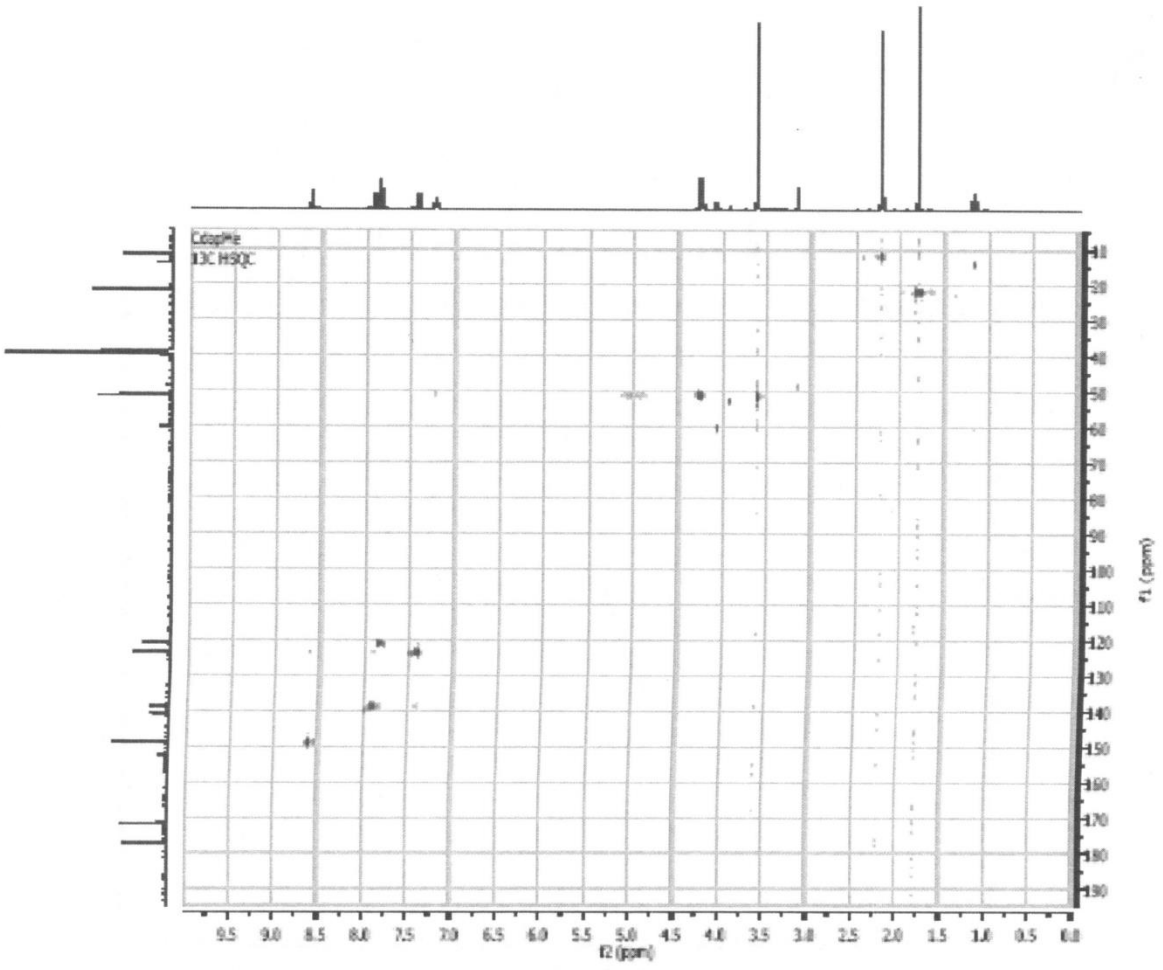

Figure S7. $^{1}H–^{13}C$ HSQC NMR spectrum of **1** in DMSO-d_6.

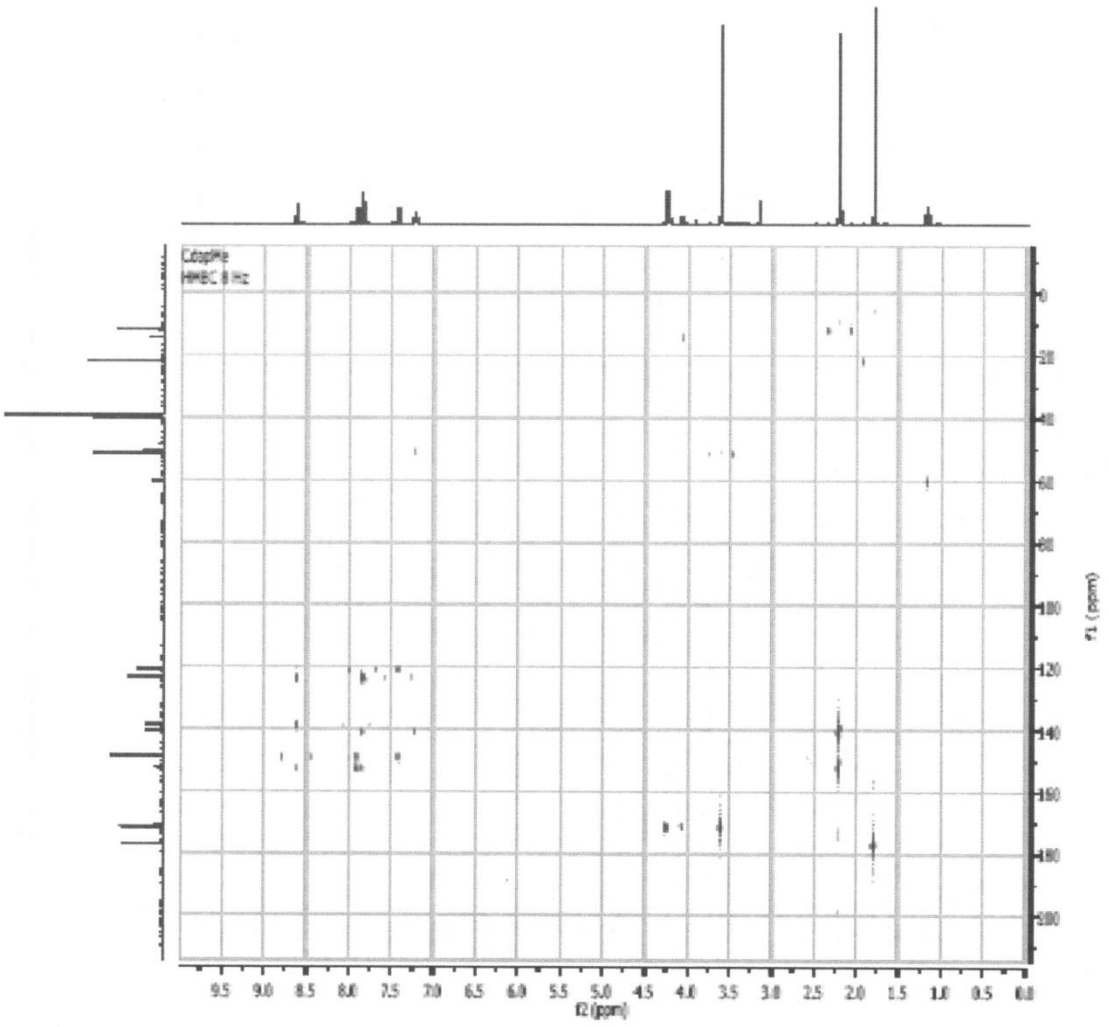

Figure S8. $^{1}H–^{13}C$ HMBC NMR spectrum of **1** in DMSO-d_6.

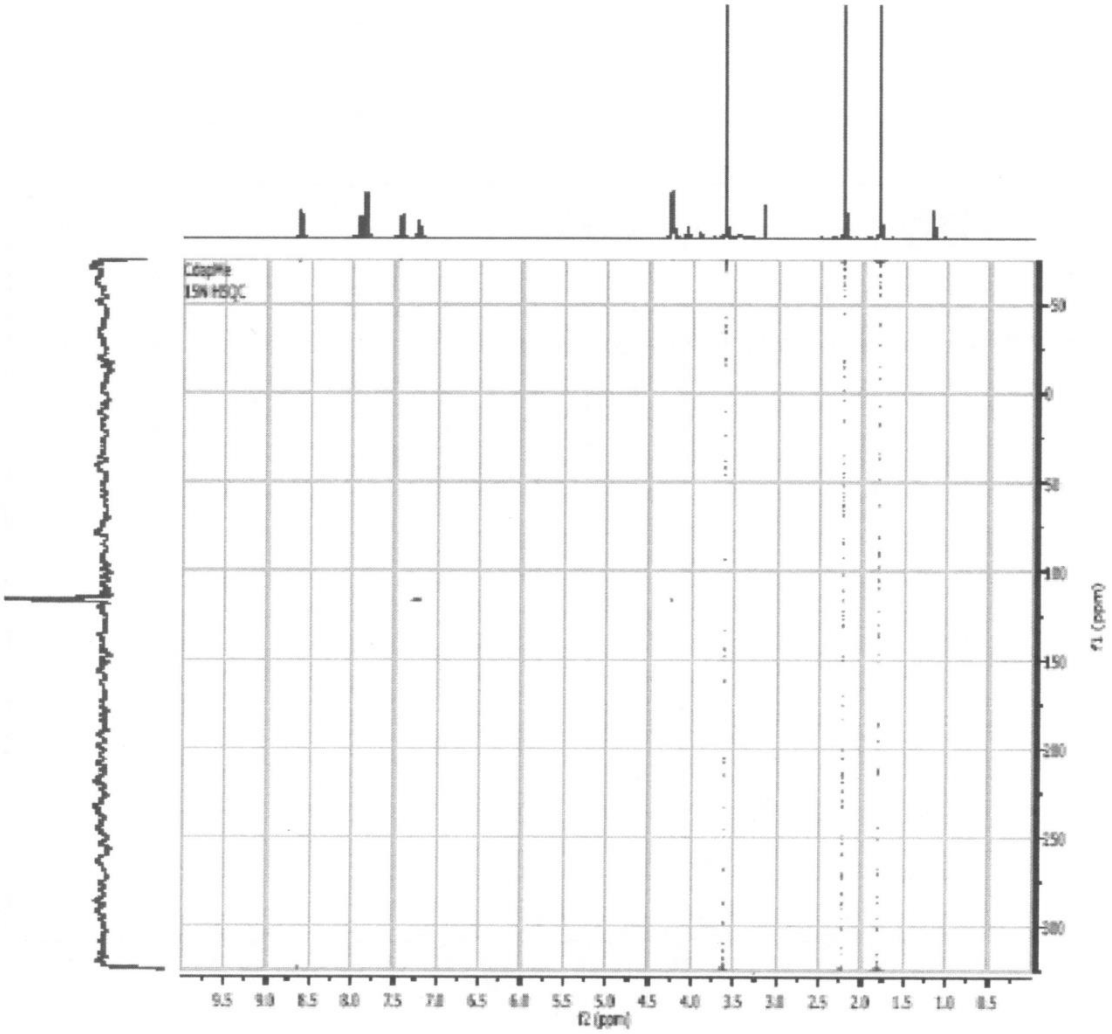

Figure S9. $^{1}H–^{15}N$ HSQC NMR spectrum of **1** in DMSO-d_6.

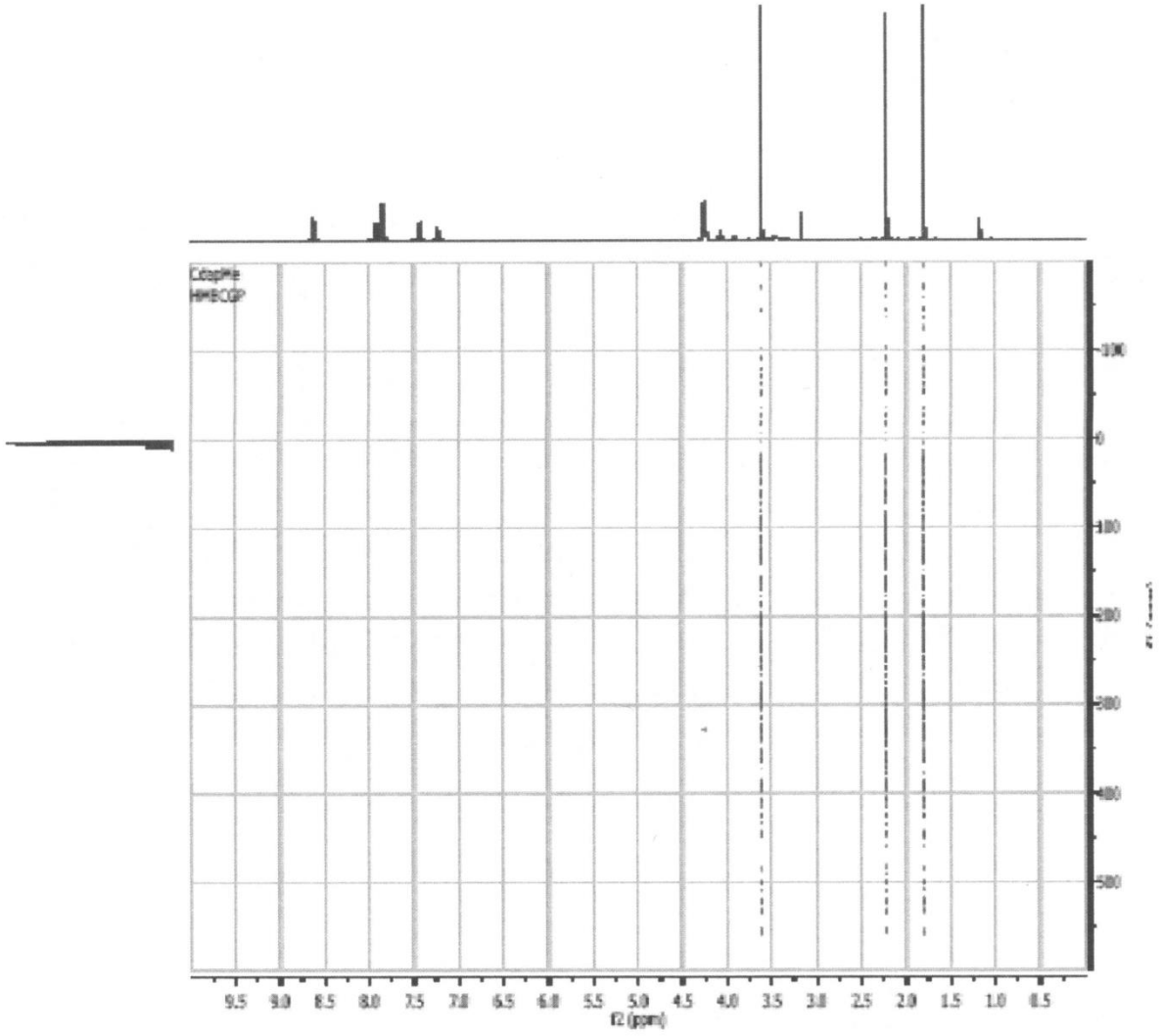

Figure S10. $^{1}H–^{15}N$ HMBC NMR spectrum of **1** in DMSO-d_6.

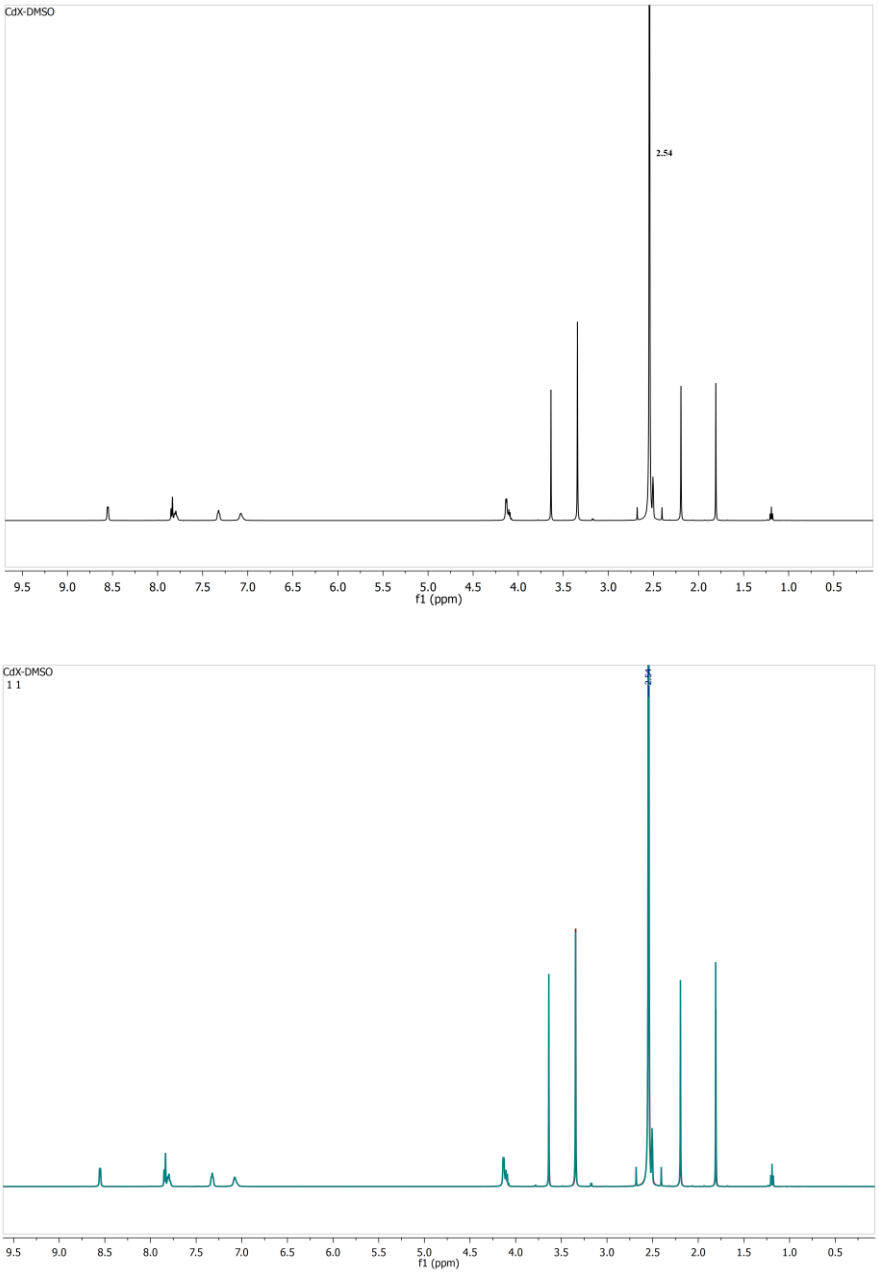

Figure S11. ^{1}H NMR spectrum of **1** in DMSO-d_6 with addition of 5 % (v) DMSO (top) and superimposed spectra of freshly prepared sample and sample after 24 h (bottom).

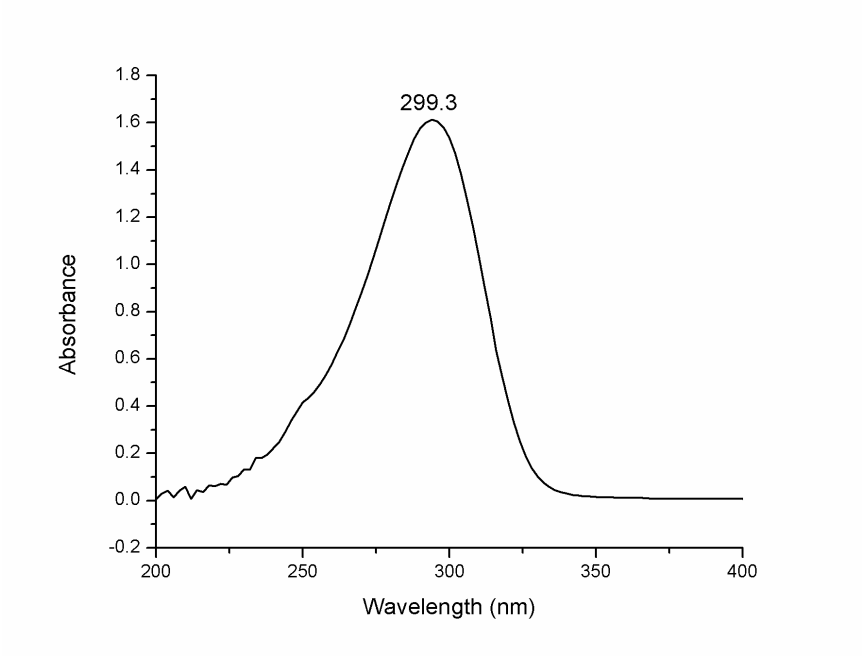

Figure S12. UV-Vis spectrum of **1** in DMSO

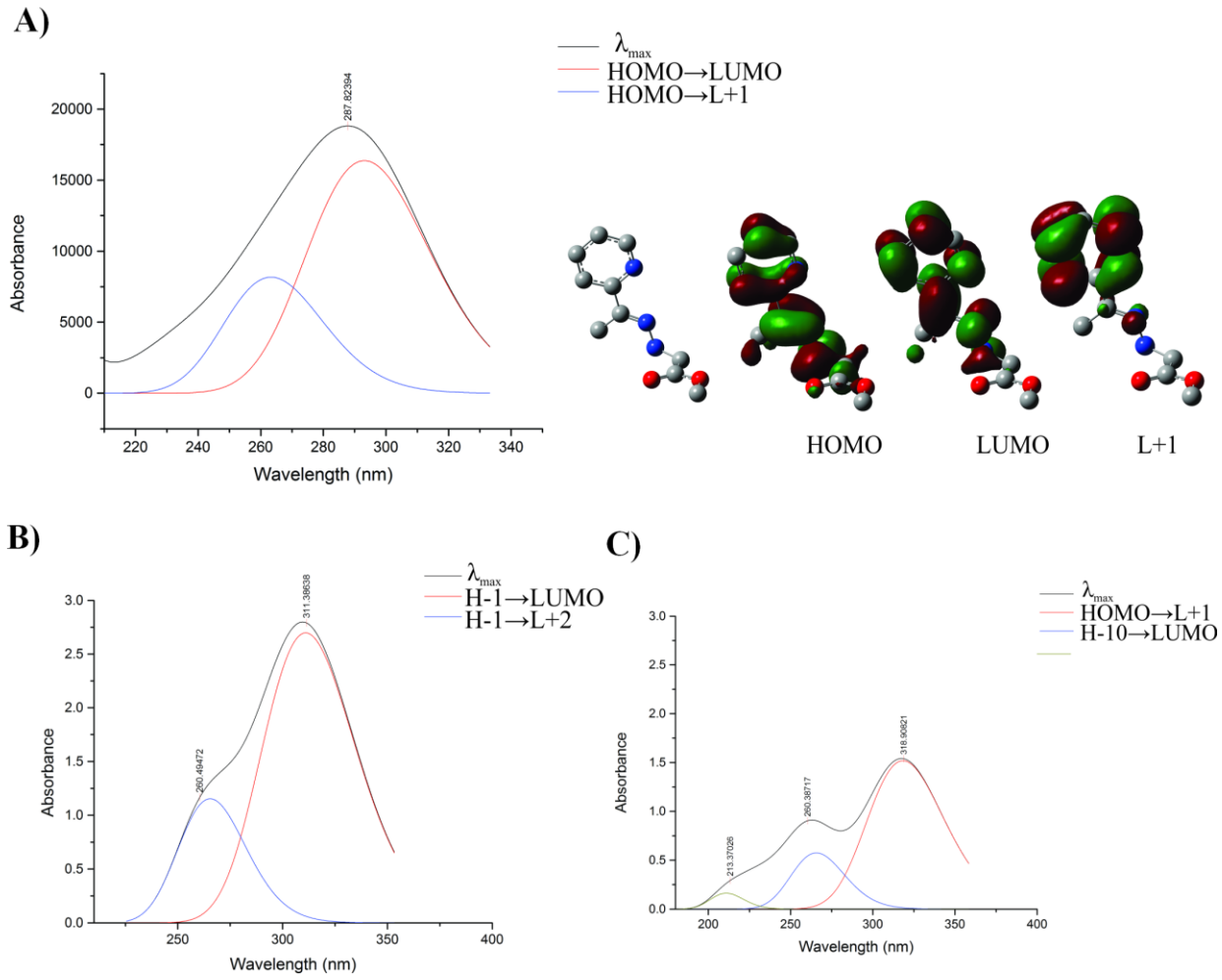

Figure S13. Calculated UV-Vis spectra for several species that can exist in DMSO solution of **1**: free aphaOMe ligand (A), binuclear complex **1** (B) and mononuclear pentacoordinated Cd(II) complex (C).

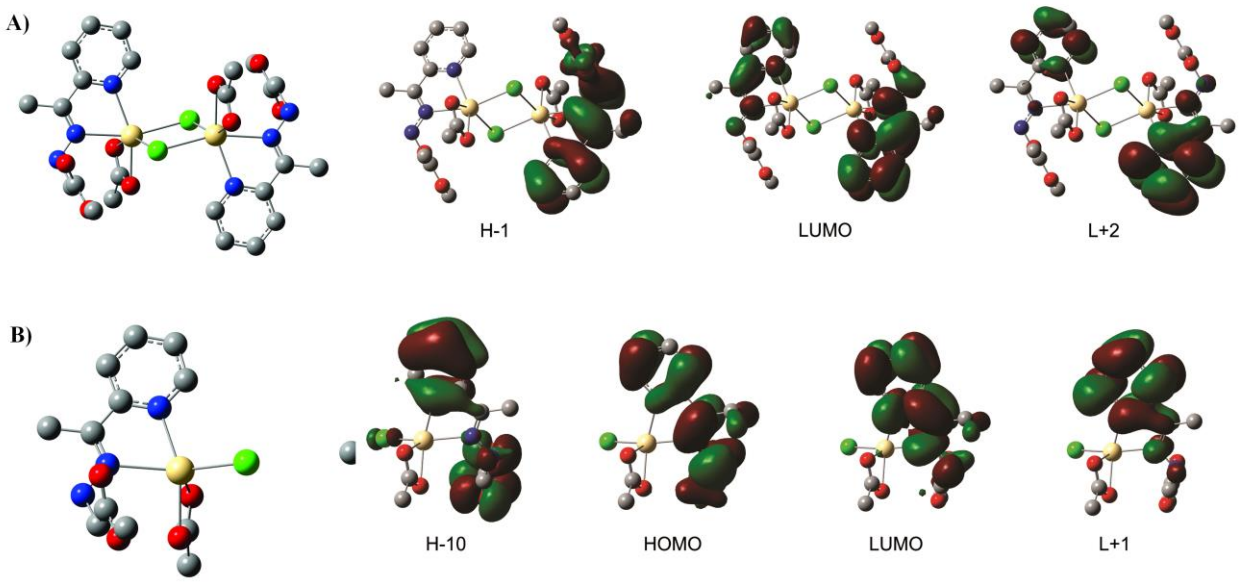

Figure S14. Optimized geometries of investigated Cd-species with calculated molecular orbitals composition: binuclear complex **1** (A) and mononuclear pentacoordinated Cd(II) monomer (B) , in DMSO solvent.

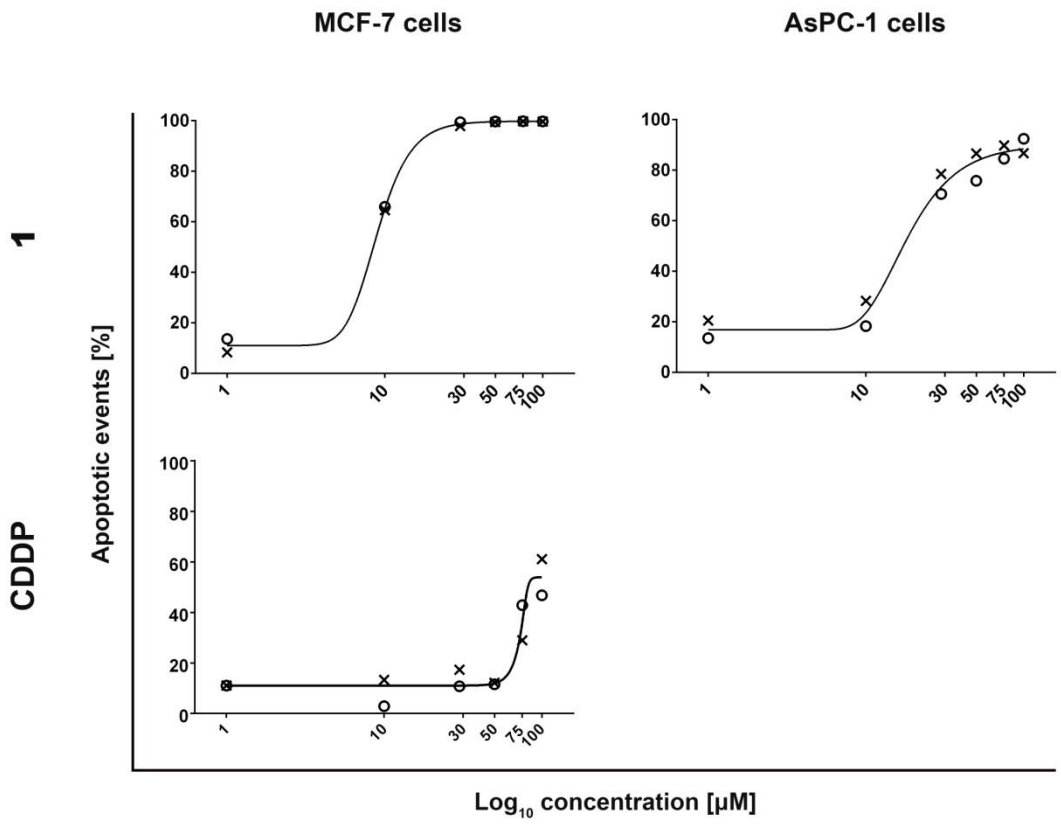

Figure S15. Concentration-response curves for investigated compounds.

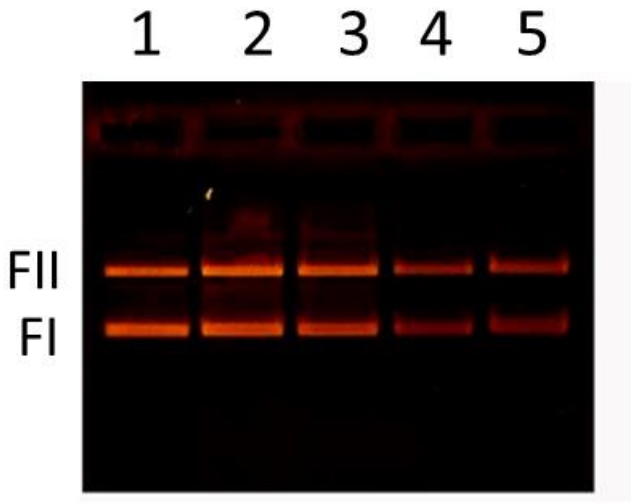

Figure S16. Agarose gel electrophoresis of reaction of pUC19 by **1**. The reaction was investigated by incubation for 90 min of 0.5 μg plasmid in 20 μL of 40 mM bicarbonate buffer pH 8.4 at 37 °C, with different concentrations of the complex. Lane 1 – control plasmid; lanes 2, 3, 4, and 5: plasmid with 0.015, 0.02, 0.03 and 0.04 mM concentration of **1**, respectively.

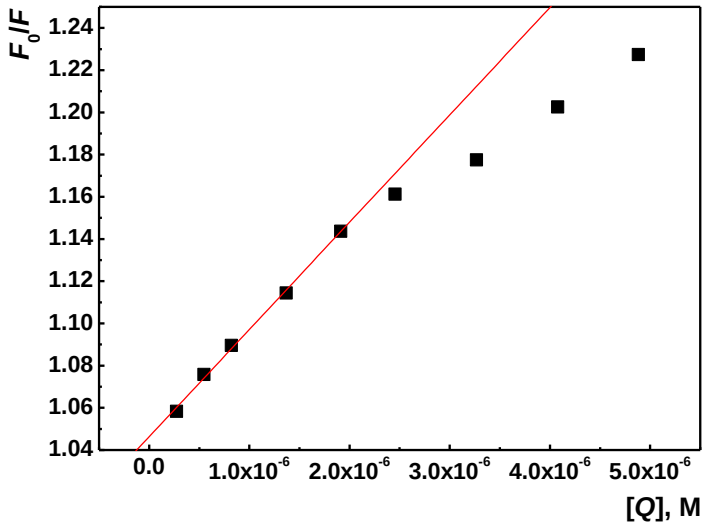

Figure S17. S-V plot for binding of **1** to HSA (c = 5 × 10^{-7} M) at 25 °C. Addition of **1** in concentration range from 0 to 4.5 × 10^{-6} M; pH = 7.35 (PBS).

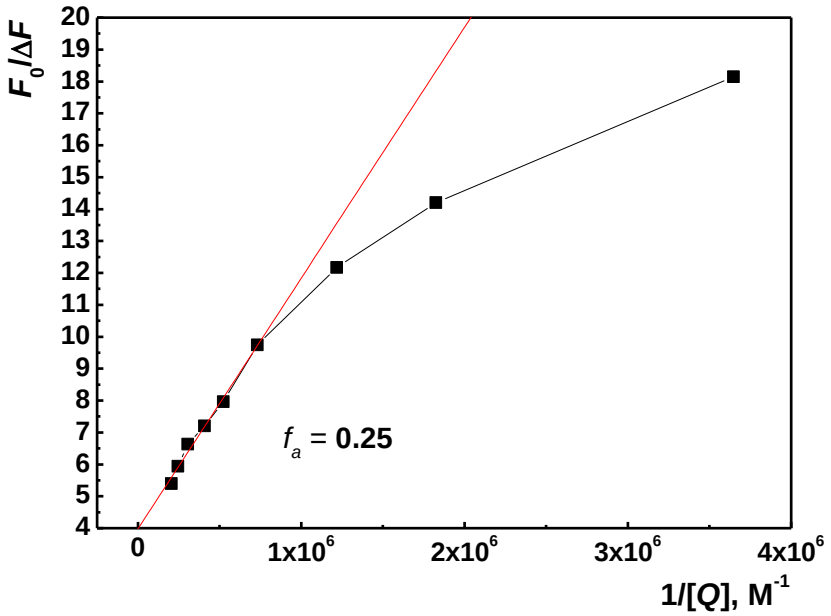

Figure S18. Modified S-V plot for binding of **1** to HSA at 25 °C; *c* (HSA) = 5 × 10^{-7} M, *c* (**1**) = 0.0 –4.5 × 10^{-6} M; pH = 7.35 (PBS).

Table S1. Interaction energies based on CE-HF energy model.

Cg···*Cg*[a] / Å	Symmetry operation[b]	Interaction energies[c], kJ mol^{-1}				
		E_{ele}	E_{pol}	E_{disp}	E_{rep}	E_{tot}
8.98	*x*+1, *y*, *z*	−105.1	−34.5	−97.8	74.1	−157.6
8.98	*x*−1, *y*, *z*	−105.1	−34.5	−97.8	74.1	−157.6
10.12	−*x*+5/2, *y*+1/2, −*z*+3/2	−62.9	−25.1	−60.9	43.5	−100.0
10.12	−*x*+5/2, *y*−1/2, −*z*+3/2	−62.9	−25.1	−60.9	43.5	−100.0
10.12	−*x*+3/2, *y*+1/2, −*z*+1/2	−62.9	−25.1	−60.9	43.5	−100.0
10.12	−*x*+3/2, *y*−1/2, −*z*+1/2	−62.9	−25.1	−60.9	43.5	−100.0
13.16	*x*, *y*+1, *z*	3.0	−0.8	−19.4	7.9	−8.6
13.16	*x*, *y*−1, *z*	3.0	−0.8	−19.4	7.9	−8.6
10.89	−*x*+3/2, *y*+1/2, −*z*+3/2	5.5	−3.9	−11.9	3.5	−4.8
10.89	−*x*+3/2, *y*−1/2, −*z*+3/2	5.5	−3.9	−11.9	3.5	−4.8
10.89	−*x*+5/2, *y*+1/2, −*z*+1/2	5.5	−3.9	−11.9	3.5	−4.8
10.89	−*x*+5/2, *y*−1/2, −*z*+1/2	5.5	−3.9	−11.9	3.5	−4.8
15.74	−*x*+1/2, *y*+1/2, −*z*+1/2	4.1	−0.9	−5.0	0.8	−0.2
15.74	−*x*+1/2, *y*−1/2, −*z*+1/2	4.1	−0.9	−5.0	0.8	−0.2
15.74	−*x*+7/2, *y*+1/2, −*z*+3/2	4.1	−0.9	−5.0	0.8	−0.2
15.74	−*x*+7/2, *y*−1/2, −*z*+3/2	4.1	−0.9	−5.0	0.8	−0.2
13.72	*x*, *y*, *z*+1	0.7	−0.6	−8.2	9.0	0.3
13.72	*x*, *y*, *z*−1	0.7	−0.6	−8.2	9.0	0.3

[a]*Cg*···*Cg* is the distance between centroids of the two interacting dimers.

[b]Symmetry operations given generate only half of the interacting molecule, as they are related to the asymmetric unit.

[c]Total energies for CE-HF benchmarked energy model (based on HF/3-21G monomer electron densities) are the sum of the four energy components, scaled appropriately:

$E_{tot} = k_{ele}E_{ele} + k_{pol}E_{pol} + k_{disp}E_{disp} + k_{rep}E_{rep}$. Scale factor have values: k_{ele} = 1.019, k_{pol} = 0.651, k_{disp} = 0.901, k_{rep} = 0.811.

Table S2. ChemPLP docking score of for binding of **1** to the DNA and HSA three binding sites

Binding site (PDB code)	**ChemPLP docking score (TOTAL_SCORE)**
IB (4LB2)	–80.72
IIA (3LU7)	–83.50
IIIA (2BXE)	–81.09
DNA (3U2N)	–52.66

References

[S1] M.J. Frisch, G.W. Trucks, H.B. Schlegel, G.E. Scuseria, M.A. Robb, G. Cheeseman, J. R. Scalmani, V. Barone, B. Mennucci, G.A. Petersson, H. Nakatsuji, M. Caricato, X. Li, H.P. Hratchian, A.F. Izmaylov, J. Bloino, G. Zheng, J.L. Sonnenberg, M. Hada, M. Ehara, K. Toyota, R. Fukuda, J. Hasegawa, M. Ishida, T. Nakajima, Y. Honda, O. Kitao, H. Nakai, T. Vreven, J. Montgomery, J. A., J.E. Peralta, F. Ogliaro, M. Bearpark, J.J. Heyd, E. Brothers, K.N. Kudin, V.N. Staroverov, R. Kobayashi, J. Normand, K. Raghavachari, A. Rendell, J.C. Burant, S.S. Iyengar, J. Tomasi, M. Cossi, N. Rega, J.M. Millam, M. Klene, J.E. Knox, J.B. Cross, V. Bakken, C. Adamo, J. Jaramillo, R. Gomperts, R.E. Stratmann, O. Yazyev, A.J. Austin, R. Cammi, C. Pomelli, J.W. Ochterski, R.L. Martin, K. Morokuma, V.G. Zakrzewski, G.A. Voth, P. Salvador, J.J. Dannenberg, S. Dapprich, A.D. Daniels, Ö. Farkas, J.B. Foresman, J. V. Ortiz, J. Cioslowski, D.J. Fox, Gaussian 09, Revision D.01, (2016).

[S2] A.D. Becke, Density-functional thermochemistry. III. The role of exact exchange, J. Chem. Phys. 98 (1993) 5648–5652. doi:10.1063/1.464913.

[S3] C. Lee, W. Yang, R.G. Parr, Development of the Colle-Salvetti correlation-energy formula into a functional of the electron density, Phys. Rev. B. 37 (1988) 785–789. doi:10.1103/PhysRevB.37.785.

[S4] A. V. Marenich, C.J. Cramer, D.G. Truhlar, Universal Solvation Model Based on Solute Electron Density and on a Continuum Model of the Solvent Defined by the Bulk Dielectric Constant and Atomic Surface Tensions, J. Phys. Chem. B. 113 (2009) 6378–6396. doi:10.1021/jp810292n.

[S5] P.J. Hay, W.R. Wadt, *Ab initio* effective core potentials for molecular calculations. Potentials for K to Au including the outermost core orbitals, J. Chem. Phys. 82 (1985) 299–310. doi:10.1063/1.448975.

[S6] P.C. Hariharan, J.A. Pople, The influence of polarization functions on molecular orbital hydrogenation energies, Theor. Chim. Acta. 28 (1973) 213–222. doi:10.1007/BF00533485.

[S7] M.M. Francl, W.J. Pietro, W.J. Hehre, J.S. Binkley, M.S. Gordon, D.J. DeFrees, J.A.

Pople, Self-consistent molecular orbital methods. XXIII. A polarization-type basis set for second-row elements, J. Chem. Phys. 77 (1982) 3654–3665. doi:10.1063/1.444267.

[S8] J. Sambrook, E.F. Fritsch, T. Maniatis, Molecular cloning: a laboratory manual, 2nd ed., Cold Spring Harbor Laboratory Press, New York, 1989.

[S9] M.E. Reichmann, S.A. Rice, C.A. Thomas, P. Doty, A Further Examination of the Molecular Weight and Size of Desoxypentose Nucleic Acid, J. Am. Chem. Soc. 76 (1954) 3047–3053. doi:10.1021/ja01640a067.

[S10] J.R. Lakowicz, G. Weber, Quenching of fluorescence by oxygen. Probe for structural fluctuations in macromolecules, Biochemistry. 12 (1973) 4161–4170. doi:10.1021/bi00745a020.

[S11] N.R. Filipović, I. Marković, D. Mitić, N. Polović, M. Milčić, M. Dulović, M. Jovanović, M. Savić, M. Nikšić, K. Anđelković, T. Todorović, A Comparative Study of In Vitro Cytotoxic, Antioxidant, and Antimicrobial Activity of Pt(II), Zn(II), Cu(II), and Co(III) Complexes with *N* -heteroaromatic Schiff Base (*E*)-2-[*N* ′-(1-pyridin-2-yl-ethylidene)hydrazino]acetate, J. Biochem. Mol. Toxicol. 28 (2014) 99–110. doi:10.1002/jbt.21541.

[S12] J.J.P. Stewart, Optimization of parameters for semiempirical methods V: Modification of NDDO approximations and application to 70 elements, J. Mol. Model. 13 (2007) 1173–1213. doi:10.1007/s00894-007-0233-4.

[S13] J. J. P. Stewart, Stewart Computational Chemistry, MOPAC2016, (2016).

[S14] O. Korb, T. Stützle, T.E. Exner, PLANTS: Application of Ant Colony Optimization to Structure-Based Drug Design, in: M. Dorigo, L.M. Gambardella, M. Birattari, A. Martinoli, R. Poli, T. Stützle (Eds.), Ant Colony Optimization and Swarm Intelligence. ANTS 2006. Lecture Notes in Computer Science, vol 4150. Springer, Berlin, Heidelberg 2006: pp. 247–258. doi:10.1007/11839088_22.

[S15] O. Korb, T. Stützle, T.E. Exner, An ant colony optimization approach to flexible protein–ligand docking, Swarm Intell. 1 (2007) 115–134. doi:10.1007/s11721-007-0006-9.

[S16] O. Korb, T. Stützle, T.E. Exner, Empirical Scoring Functions for Advanced Protein−Ligand Docking with PLANTS, J. Chem. Inf. Model. 49 (2009) 84–96. doi:10.1021/ci800298z.

[S17] A. Pedretti, L. Villa, G. Vistoli, VEGA - an open platform to develop chemo-bioinformatics applications, using plug-in architecture and script programming, J. Comput. Aided. Mol. Des. 18 (2004) 167–73.